International Journal of Technical Innovation in Modern Engineering & Science (IJTIMES)
Impact Factor: 5.22 (SJIF-2017), e-ISSN: 2455-2585
Volume 5, Issue 07, July-2019

PLL TECHNIQUES FOR DISTRIBUTED GENERATION SYSTEMS UNDER GRID ABNORMAL CONDITIONS

G CHANDRA SEKHAR[1]

Assistant Professor, Dept of EEE, Tirumala Engineering College Medchal Distirict, Hyderabad, Telangana-501301, India,

Abstract – ***In this project, the synchronization of grid voltage of the distributed generation systems are studied by the considering numerous grid synchronization techniques. so as to urge the desired quantity of correct and quick grid voltage synchronization algorithms this is often vital to figure underneath distorted and unbalanced conditions. thus it's necessary to investigate the synchronization capability of 3 advanced synchronization systems: the three-phase enhanced PLL the decoupled double synchronous reference frame phase-locked loop (PLL), and therefore the dual second order generalized integrator PLL that is enforced underneath such conditions. The fuzzy controller is that the most fitted for the human decision-making mechanism, providing the operation of associate electronic system with decisions of experts. Here we tend to are exploitation the fuzzy controller compared to different controllers. Here we tend to are exploitation the fuzzy controller compared to different controllers for higher performance. furthermore if different system depend on frequency-locked loops have additionally been developed, PLLs are chosen because of their link with dq0 controllers. By exploitation MATLAB/Simulink code the simulation are done.***

Keywords: Electric variable measurements, electrical engineering, frequency estimation, harmonic analysis, monitoring, synchronization, Fuzzy logic controller

I. INTRODUCTION

The power share of renewable energy-based generation systems is meant to achieve 20% by 2030, wherever wind and photovoltaic (PV) systems are assumed to be the foremost outstanding samples of integration of such systems within the electrical network [1].The augmented penetration of those technologies within the electrical network has bolstered the already existing concern among the transmission system operators (TSOs) regarding their influence within the grid stability; as a consequence, the grid affiliation standards have become a lot of and a lot of restrictive for distribution generation systems altogether countries [2]–[6].In the actual grid code necessities (GCRs), special constraints for the operation of such plants below grid voltage fault conditions have gained an excellent importance. These necessities confirm the fault boundaries among those through that a grid-connected generation system shall stay connected to the network, giving rise to specific voltage profiles that specify the depth and clearance time of the voltage sags that they need to face up to. Such necessities are referred to as low voltage ride through (LVRT) and are represented by a voltage versus time characteristic [7]. Although the LVRT necessities varied standards ar terribly totally different, as shown in [8-10], the primary issue that generation systems should afford once voltage sag happens is that the limitation of their transient response, so as to avoid its protecting disconnection from the network. this can be the case, for example, of fastened speed wind turbines supported squirrel cage induction generators, wherever the fall within the stator windings will conduct the generator to an over speed tripping, as shown in [11-12]. Likewise, variable speed wind generation systems could lose controllability within the injection of active/reactive power thanks to the disconnection of the rotor side converter underneath such conditions [13-14]. In any case, a quick detection of the fault contributes to rising the consequences of those solutions; thus, the synchronization algorithms are crucial.

These solutions are supported advanced control systems that require to own correct data of the grid voltage variables so as to figure properly, something that has prompted the importance of grid synchronization algorithms. In power systems, the synchronous reference frame PLL (SRF PLL) is that the most extended technique for synchronizing with three-phase systems. all the same, despite the actual fact that the performance of SRFPLL is satisfactory underneath balanced conditions, its response is inadequate underneath unbalanced, faulty, or distorted conditions.

In this work, three improved and advanced grid synchronization systems are studied and evaluated: the decoupled double synchronous reference frame PLL (DDSRF PLL) the dual second order generalized integrator PLL (DSOGI PLL), and also the three-phase enhanced PLL (3phEPLL) . Their performance, procedure price, and dependability of the amplitude and phase detection of the positive sequence of the voltage, underneath unbalanced and distorted.

II.GRID SYNCHRONIZATION BASED ON GCR

Even though many works are revealed among the sphere of grid synchronization, the majority of them are focused on analyzing the individual dynamic performance of every proposal, while not initial decisive a time response window among the dynamic behaviour of the system underneath take a look at, which might be thought of to be satisfactory.

III.SYNCHRONIZATION S YSTEMS

Many of the positive-sequence detection algorithms are supported SRF PLLs. Despite having a good response beneath balanced conditions, their performance becomes low in unbalanced faulty grids (95% of cases), and their smart operation is extremely conditioned to the frequency stability, that is incompatible with the concept of a sturdy synchronizationsystem.

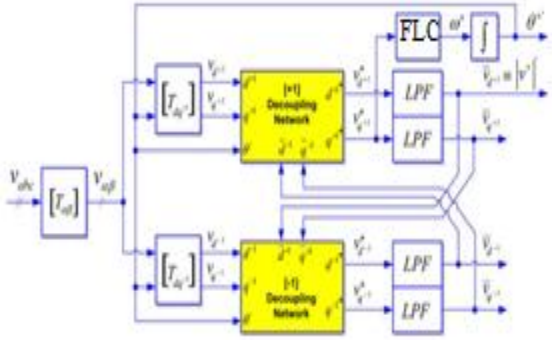

Fig.1. DDSRF-PLL block diagram

In the framework of those topologies, 3 PLL structures are mentioned and evaluated during this project.

3.1 DDSRF PLL

The DDSRF PLL that is enforced for the improving the standard SRF PLL. This synchronization system exploits two synchronous reference frames rotating at the fundamental utility frequency, one counterclockwise and another one clockwise , so as to realize an correct detection of the positive- and negative-sequence elements of the gridsvoltage vector once it's stricken by unbalanced grid faults. The diagram of the DDSRF PLL is shown in Fig.1.When the three-phase grid voltage is unbalanced, the basic positive-sequence voltage vector seems as a dc voltageon the dq+1 axes of the positive-sequence SRF and as acvoltages at doubly the fundamental utility frequency on the dq−1axes of the negative-sequence SRF Low-pass filters (LPFs) inFig. three are answerable for extracting the dc component fromthe signal on the decoupled SRF axes.

Finally, the PI controller of the DDSRF PLL works on thedecoupled q-axis signal of the positive-sequence SRF (v∗q+1)and performs a similar operate as in an SRF PLL, positioning thepositive-sequence voltage with the d-axis.

3.2 DSOGI PLL

The operative principle of the DSOGI PLL for estimating the positive- and negative-sequence components of the grid voltage vectors is based on using the instantaneous symmetrical component (ISC) technique on the αβ stationary frame of reference.

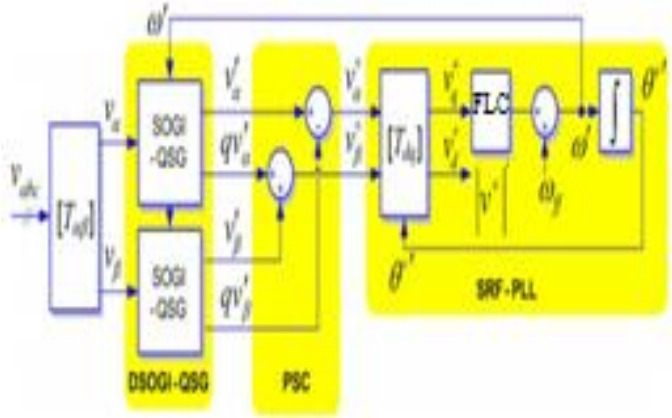

Fig. 2. DSOGI-PLL block diagram

The diagram of the DSOGI PLL is shown in Fig. 2. because it are often noticed , the ISC methodology is enforced by the positive-sequence calculation block.

3.3 3phEPLL

The enhanced phase-locked loop (EPLL) is a synchronization system that has evidenced to produce sensible results in singlephase synchronization systems. an EPLL is actually an adaptive bandpass filter, that is in a position to regulate the cutoff frequency as a function of the input signal. Its structure was later tailored for the three-phase case so as to notice the positive-sequence vector of three-phase signals, getting the 3phEPLL that's diagrammatical in Fig. 5.

IV. DISCRETE IMPLEMENTATION

The performance of the various structures underneath take a look at is really obsessed with their final digital implementation, significantly onThe discretization approach created to their continuous equations. This implementation is essential and will be studied well as a clear-cut implementation will make to extra delays within the loop that hinder the great performance of the PLL. so as to facilitate the comprehension of the method, the various building blocks that seem at Figs.1–4 are documented.

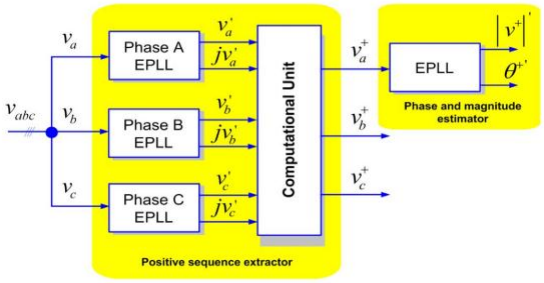

Fig. 3.3phEPLL block diagram

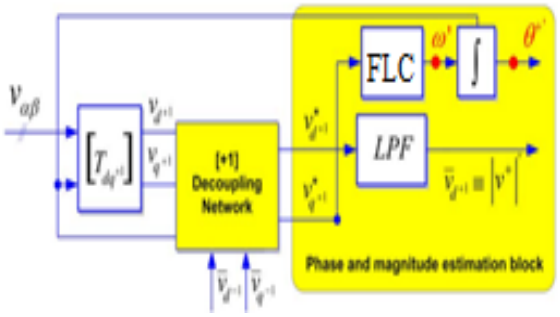

Fig. 4.Phase and magnitude estimation loop of the DDSRF PLL

4.1 DDSRF-PLL Discretization

The discrete model of this PLL will be simply obtained since the continual illustration of many elements doesn't amendment within the separate domain. this is often the case for the transformation blocks Tαβ, Tdq+1, and Tdq−1 :

1) Positive and Negative-Sequence Decoupling Networks: The decoupling network constitutes one in every of the foremost vital contributions of this synchronization methodology.

2) phase and Magnitude estimator Discretization: within the DDSRF PLL, the decoupling network seems embedded within the classical SRF-PLL loop (see Fig. 6).

$$\begin{bmatrix} v^*_{d+1}[n+1] \\ v^*_{q+1}[n+1] \end{bmatrix} = \begin{bmatrix} 1 & 0 \\ 0 & 1 \end{bmatrix} \cdot \begin{bmatrix} v_{d+1}[n+1] \\ v_{q+1}[n+1] \end{bmatrix} + \begin{bmatrix} -cos(2\theta'[n]) & -sin(2\theta'[n]) \\ sin(2\theta'[n]) & -cos(2\theta'[n]) \end{bmatrix} \cdot \begin{bmatrix} \bar{v}_{d-1[n]} \\ \bar{v}_{q-1[n]} \end{bmatrix} \times \begin{bmatrix} v^*_{d-1[n+1]} \\ v^*_{q-1[n+1]} \end{bmatrix} =$$
$$\begin{bmatrix} 1 & 0 \\ 0 & 1 \end{bmatrix} \cdot \begin{bmatrix} v_{d-1}[n+1] \\ v_{q-1}[n+1] \end{bmatrix} + \begin{bmatrix} -cos(-2\theta'[n]) & -sin(-2\theta'[n]) \\ sin(-2\theta'[n]) & -cos(-2\theta'[n]) \end{bmatrix} \cdot \begin{bmatrix} \bar{v}_{d+1[n]} \\ \bar{v}_{q+1[n]} \end{bmatrix} \quad (1)$$

The distinct controller and therefore the measuring device is engineered employing a backward numerical approximation. The frequency and part will then be drawn within the z-domain (2), considering v∗q+1 because the error to be decreased . during this equation, a feedforward of the nominal frequency is given by means that of ωff

$$W'(z) = \frac{(k_p + k_i.T_s)z - k_p}{z-1} . V^*_{q+1}(z) + \omega ff\theta^{+\prime} = \frac{T_s.z}{z-1} . W'(z) \quad (2)$$

Finally, sample-based illustration provides rise to (3), that are the expressions to be enforced.

$$\omega'[n+1] = \omega'[n] - k_p . v^*_{q+1}[n] + (k_p + k_i.T_s) . V^*_{q+1}(n+1)\theta^{+\prime}[n+1] = \theta^{+\prime}[n] + T_s . \omega'[n+1] \quad (3)$$

In these equations, a frequency feed forward has been introduced as an initial condition to ω.

4.2 LPF Block Discretization:

The amplitudes of the dq positive- and negative-sequence elements are the outputs of the decoupling networks. However, four infinite impulse responses (IIR) LPFs extract the ripple from every sequence estimation so as to strengthen the performance of the PLL just in case of harmonic pollution. A first-order filter with a cutoff frequency ωf, adequate half the grid frequency, was originally proposed; therefore, a similar transfer perform has been enforced during this paper for analysis functions in

$$y[n] = \frac{1}{T_s\omega_f+1}.x[n] + \frac{T_s\omega_f}{T_s\omega_f+1}.u[n].x[n+1] = y[n] \quad (4)$$

4.3. DSOGI-PLL Discretization:

4.3.1DSOGI-QSG Block Discretization:

As was antecedently mentioned in Section II, the DSOGI-based quadrature signal generator (QSG) of Fig. 4 consists of two freelance and decoupled second-order generalized integrators (SOGIs). In Fig. 5, the block diagram of the enforced SOGI is shown

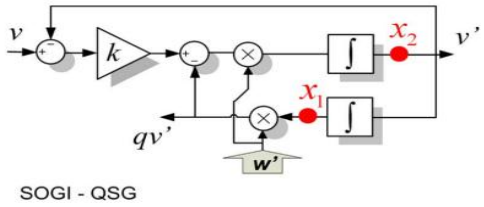

Fig.5. Quadrature signal generator based on a second order generalized integrator (SOGI QSG)

This quadrature signal generator (QSG) could be a linear system itself; so, a discrete representation will be consistently obtained if the continual state space is antecedently deducted. The equations of the SOGI state space seem elaborated in (5). wherever v constitutes the input whereas v and qv are the two inquadrature output signals

$$\left.\begin{matrix}\dot{x}_n = A.x_n + B.v \\ y_n = C.x_n\end{matrix}\right\};\ x_n = \begin{bmatrix}x_1\\x_2\end{bmatrix} y_n = \begin{bmatrix}y'\\qv'\end{bmatrix}$$
$$A = \begin{bmatrix}0 & 1\\ -\omega'^2 & -k.\omega'\end{bmatrix} B = \begin{bmatrix}0\\k.\omega'\end{bmatrix} C = \begin{bmatrix}0 & 1\\ \omega' & 0\end{bmatrix} \quad (5)$$

In these matrices, Ts is that the sampling time of the discrete system, ω[n] is that the estimated frequency magnitude, that comes from the estimation created at the SRF-PLL block at every computation step, and k is that the SOGI gain

$$X[n+1] = A'.x[n] + B'.v[n]$$
$$y[n] = c'.x[n] + D'.v[n] \quad (6)$$

Where Ts is the sampling time.

4.3.2 SRF PLL Discretization:

The frequency and phase detection is obtained by means that of the SRF PLL shown in Fig. 6.

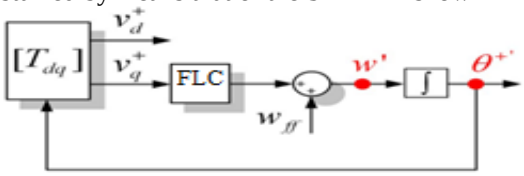

Fig. 6. State variables of the SRF-PLL block.

The discretization of the controller and therefore the integrator is performed victimization the backward numerical approximation.

$$W'(z) = \frac{(k_p+k_i.T_s)z-k_p}{z-1}.V^*_{q+1}(z) + \omega ff\theta^{+'} = \frac{T_s.z}{z-1}.W'(z) \quad (7)$$

4.3.3 3phEPLL Discretization

This three-phase grid synchronization system exploits the EPLL as a construction signal generator. an freelance EPLL is employed for process each of the three-phase voltages. Discretization: The block diagram of the EPLL enforced during this paper is bestowed in Fig. 7.

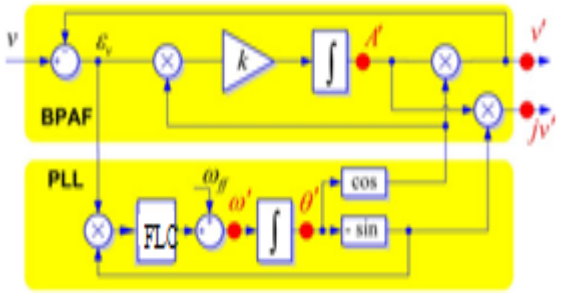

Fig. 7. Quadrature signal generator based on an EPLL structure.

According to this diagram, the state space illustration of the EPLL within the continuous domain are often written as shown in

$$\dot{A}'(t) = k.\, e(t).\cos\theta'(t)$$
$$\theta(t) = \omega'(t) + \frac{k_p}{k_1}.\,\dot{\omega}'(t) \quad (8)$$

Finally, once the state variables are calculated, the EPLL output will be obtained by generating the two quadrature signal

$$V'[n+1] = A'[n+1].\cos(\theta'[n+1])$$
$$qv'[n+1] = -A'[n+1].\sin(\theta'[n+1]) \quad (9)$$

This type of discretization methodology desires a a lot of accurate standardization, because of the actual fact that the stable regions of the s-plane and z-plane are totally different.

4.3.4 Computational Block Unit: The description for this block is that the same in each discrete and continuous domains. all the same, specific equations are utilized in this paper.

4.3.5 Phase and Magnitude Detection Block: This element is based on another EPLL, which is accountable for estimating the phase and also the magnitude of the positive-sequence fundamental element.

V.TESTING SIGNALS ANDSIMULATION SETUP

5.1 Voltage sags:

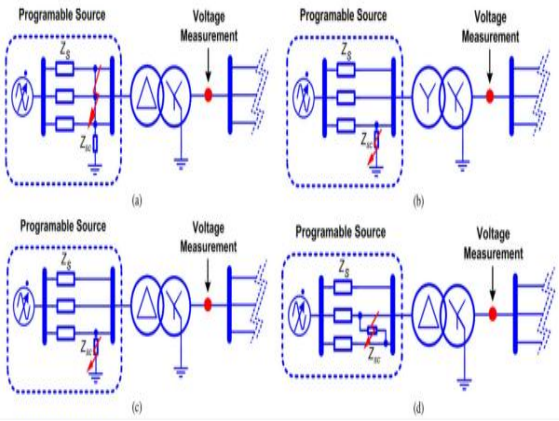

Fig. 8. Generation of grid voltage sags in the experimental setup.

That these sags are the foremost characteristic ones that have an effect on wind generation systems. In Table I, the magnitude and also the phase of the symmetrical components of the voltage throughout the fault amount are indicated in each case, presumptuous that the prefault voltage is often adequate V + =100,V− = 0, and V zero = zero.
so as to get the same dips, totally different faults are emulated with the programmable ac supply at the primary winding of the transformer, as indicated in Fig. 8.**5.2 Harmonic-polluted voltage (8% THD):**
According to the EN50160 customary, the thd of the voltage waveforms at the output of a generation facility can't be more than 8 %. Considering this demand, Table II shows the harmonic composition used for evaluating the performance of the grid synchronization systems beneath take a look at once the grid voltages become distorted

5.3 Grid voltage frequency jumps:
By means that of the programmable supply, a 10-Hz jump (from 50 to 60 Hz) within the frequency worth of the positive sequence has been applied to investigate the response of the frequency reconciling structures underneath check.

Table 1.Harmonic Composition forthe Test

Order of harmonic	THD (%)
2nd	2%
4th	1%
5th	5%
7th	4%
11th	3%
13th	3%

VI.FUZZY LOGIC CONTROLLER

In FLC, basic control action is determined by a collection of linguistic rules. These rules are determined by the system. Since the numerical variables are converted into linguistic variables, mathematical modelling of the system isn't needed in FC. The FLC contains of three parts: fuzzification, interference engine and defuzzification. The FC is characterised as i. seven fuzzy sets for every input and output. ii. Triangular membership functions for simplicity. iii. Fuzzification mistreatment continuous universe of discourse. iv. Implication mistreatment Mamdani's, 'min' operator. v. Defuzzification mistreatment the peak methodology.

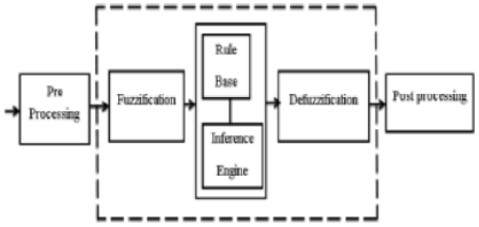

Fig. 9.Fuzzy logic controller

6.1 Fuzzification: The Partition of fuzzy subsets and therefore the form of membership cerium (k) E (k) function adapt the shape up to applicable system. the worth of input error and alter in error are normalized by an input scaling factor.

Table 2. Fuzzy Rules

Change in error	Error						
	NB	NM	NS	Z	PS	PM	PB
NB	PB	PB	PB	PM	PM	PS	Z
NM	PB	PB	PM	PM	PS	Z	Z
NS	PB	PM	PS	PS	Z	NM	NB
Z	PB	PM	PS	Z	NS	NM	NB
PS	PM	PS	Z	NS	NM	NB	NB
PM	PS	Z	NS	NM	NM	NB	NB
PB	Z	NS	NM	NM	NB	NB	NB

In this system the input scaling factor has been designed such input values are between -1 and +1. The triangular form of the membership function of this arrangement presumes that for any explicit E(k) input there's only one dominant fuzzy subset. The input error for the FLC is given as

$$E(k) = \frac{P_{ph}(k) - P_{ph}(k-1)}{V_{ph}(k) - V(k-1)} \quad (10)$$

$$CE(k) = E(k) - E(k-1) \quad (11)$$

6.2 Inference Method: several composition ways like Max–Min and Max-Dot are planned within the literature. during this paper Min technique is employed. The output membership function of every rule is given by the minimum operator and maximum operator. Table 1 shows rule base of the FLC.

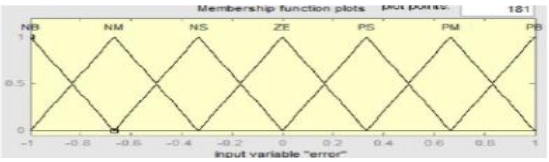

Fig.10.Membership functions

6.3 Defuzzification: As a plant sometimes requires a nonfuzzy value of control, a defuzzification stage is required. To figure the output of the FLC, „height" methodology is employed and also the FLC output modifies the control output. Further, the output of FLC controls the switch within the inverter. to realize this, the membership functions of FC are: error, change in error and output. The set of FC rules are derived from

$$u = -[\alpha E + (1-\alpha)^* c]$$

Where α is self-adjustable factor which can regulate the whole operation.

VII.SIMULATION PERFORMANCE OF THE PLLS UNDER TEST

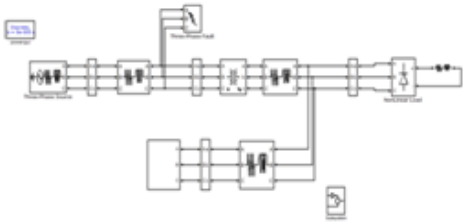

Fig. 11 General Distribution system

Fig.12 DDSRF PLL

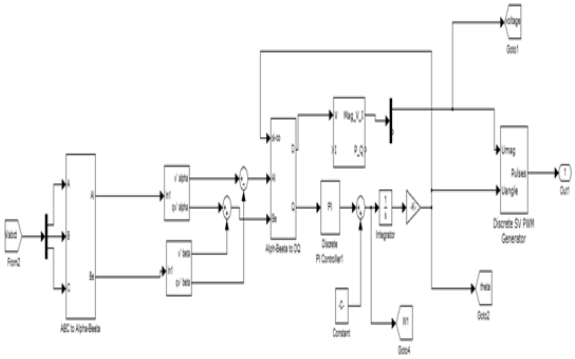

Fig.13DSOGI PLL

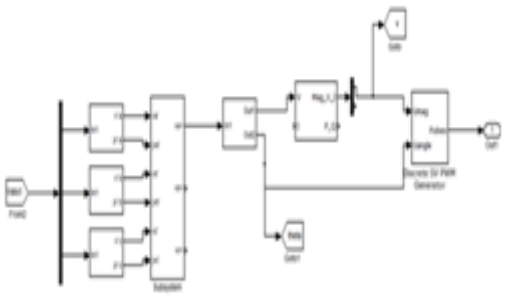

Fig.14 Three Phase EPLL

Type A Sag:

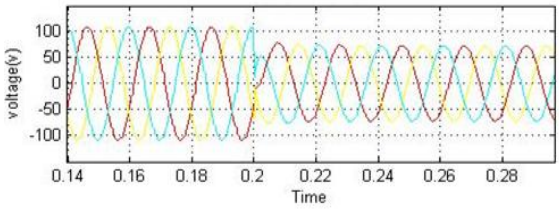

(a) input signal(v)

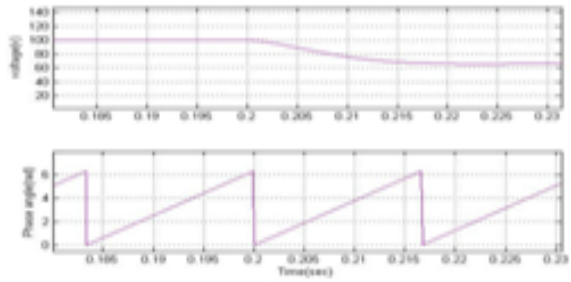

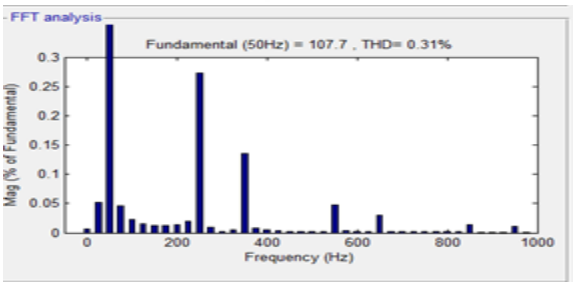

(b) DDSRF PLL

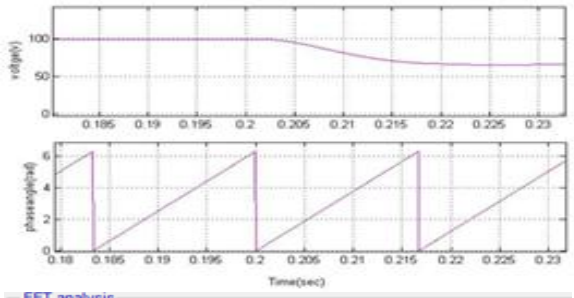

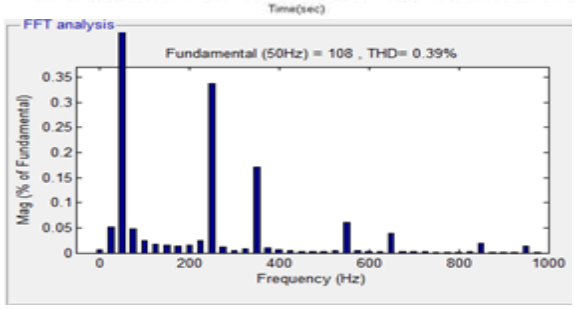

(c)DSOGI PLL

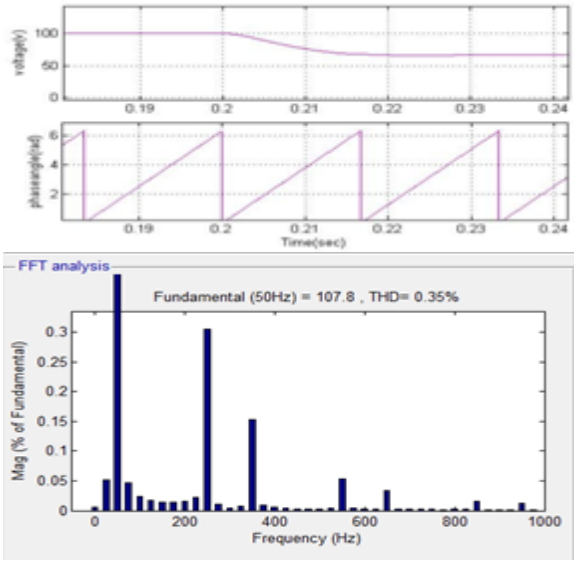

(d)EPLL

Fig.15 Amplitude (V) and phase (rad) detection for type A sag

Type B Sag

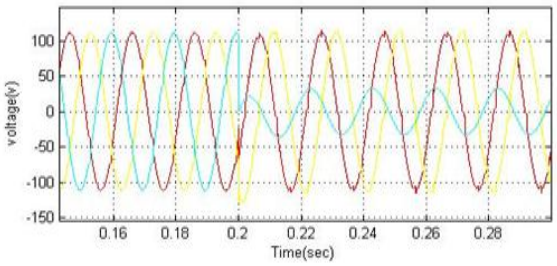

(a) Input signal(v)

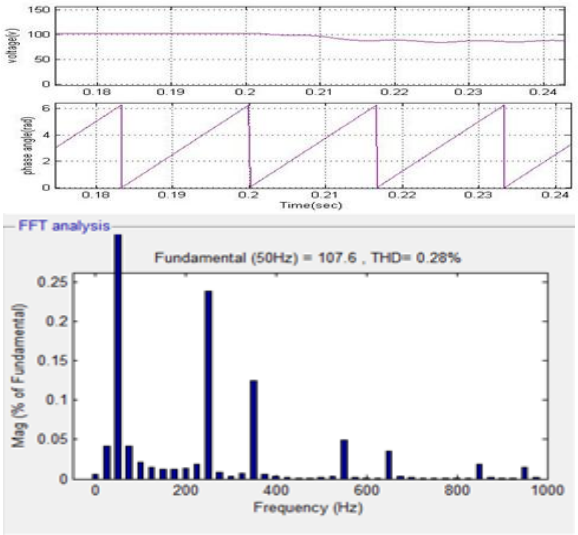

(b) DDSRF PLL

Fig.16 Amplitude (V) and phase (rad) detection for type B sag

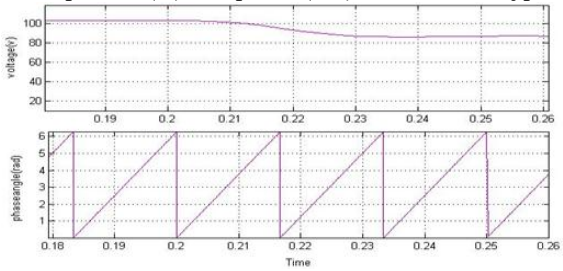

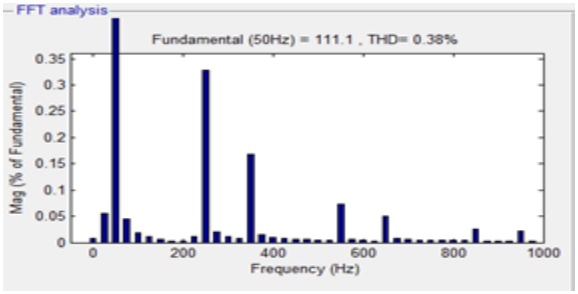

(c) DSOGI PLL

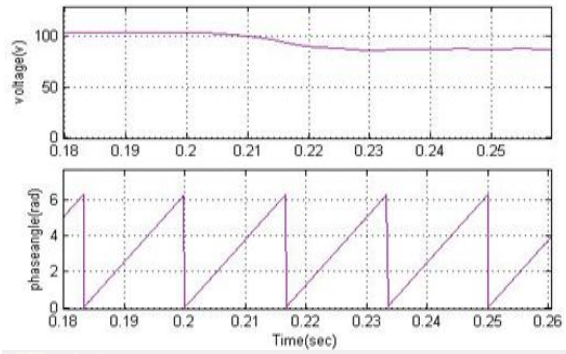

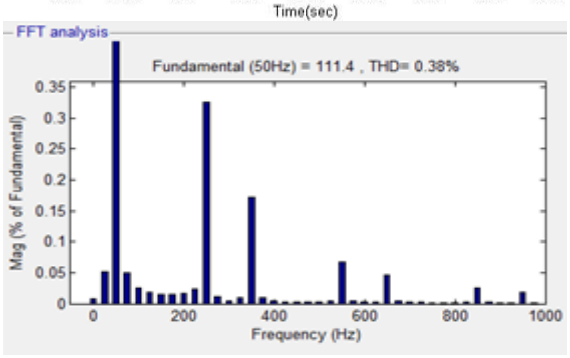

(d) EPLL

Fig.17Amplitude (V) and phase (rad) detection for type B sag

Type C Sag

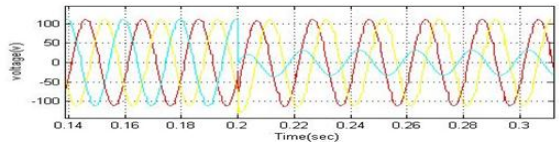

(a) Input signal (V)

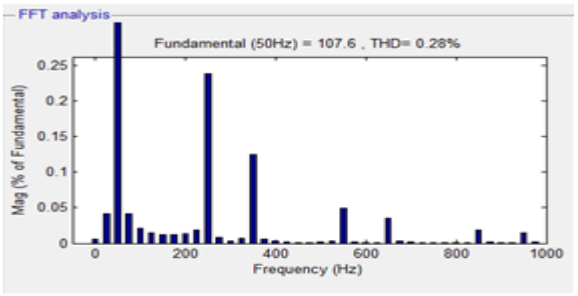

(b) DDSRF PLL

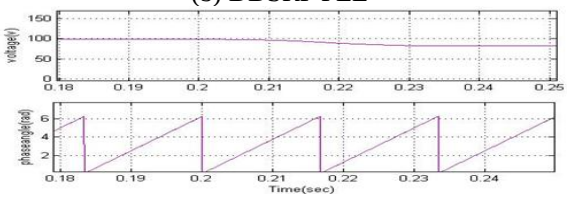

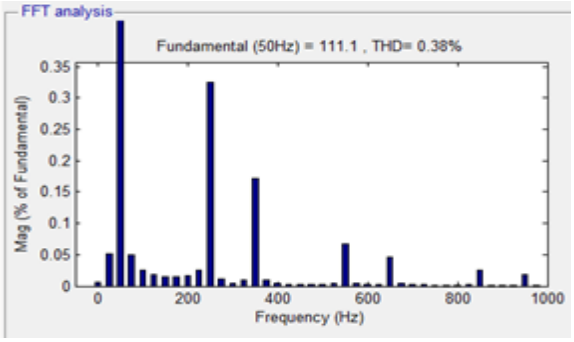

(c) DSOGI PLL

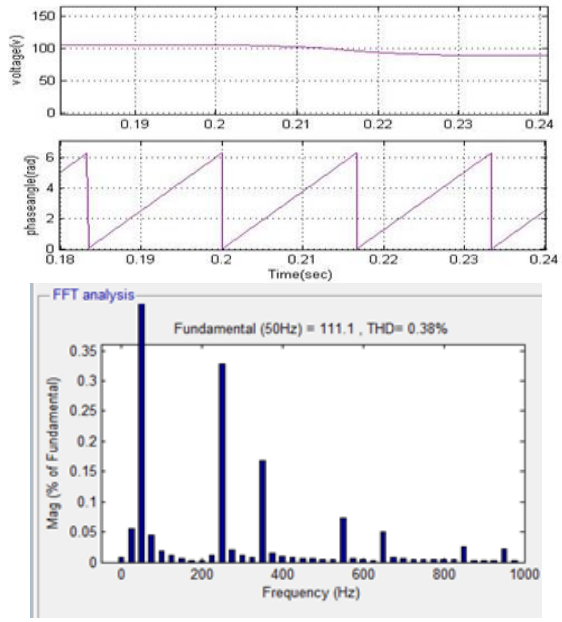

(d) EPLL

Fig.18 Amplitude (V) and phase (rad) detection for type C sag

Type D sag

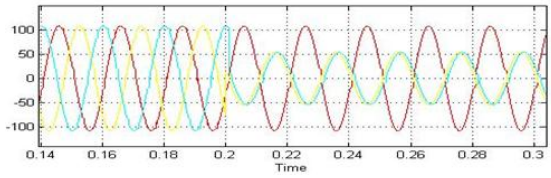

(a) Inputsignal (v)

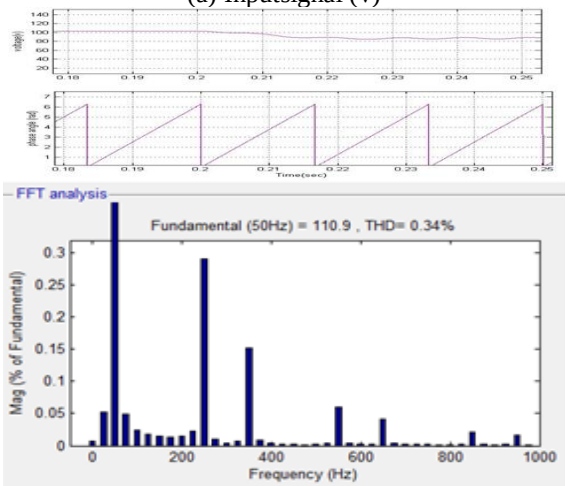

(b) DDSRF PLL

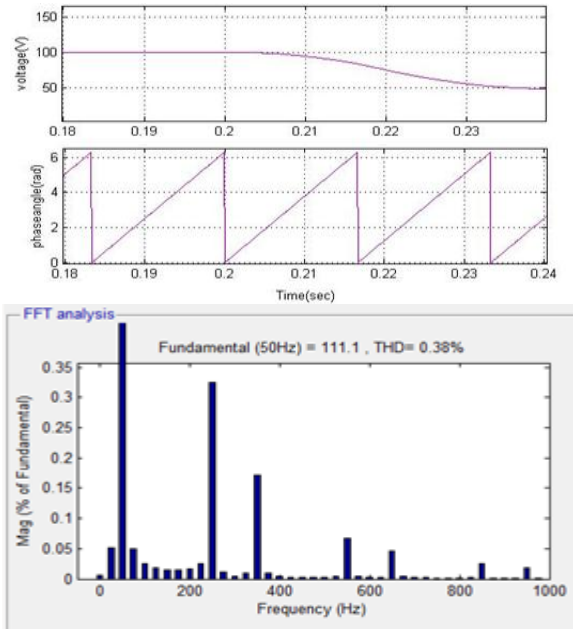

(c) DSOGI PLL

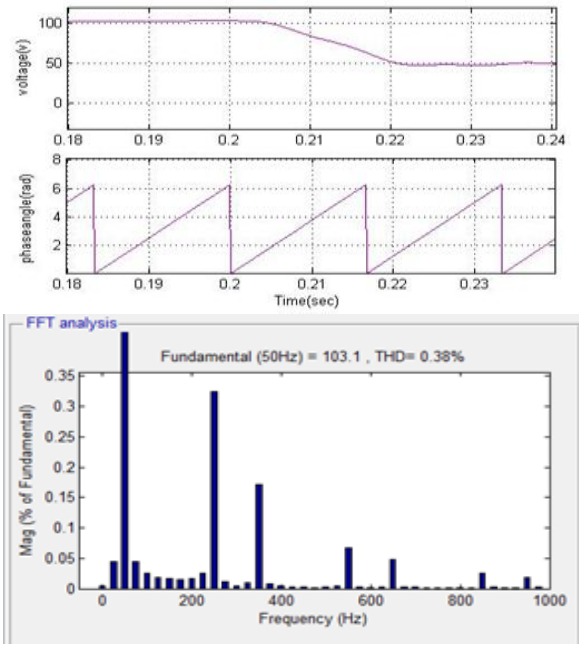

(d) EPLL

Fig. 19 Amplitude (V) and phase (rad) detection for type D sag

Behavior of PLLs in Case of Frequency Changes (50–60 Hz)

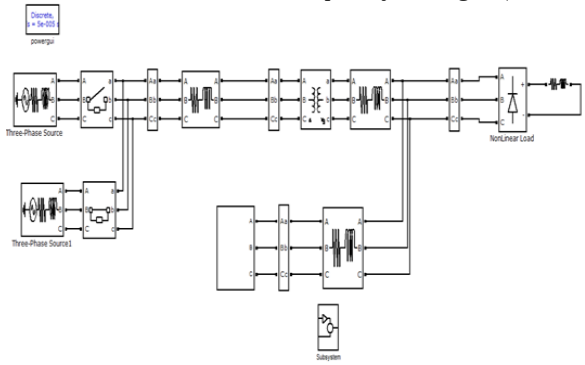

Fig.20 General Distribution system when Frequency changes

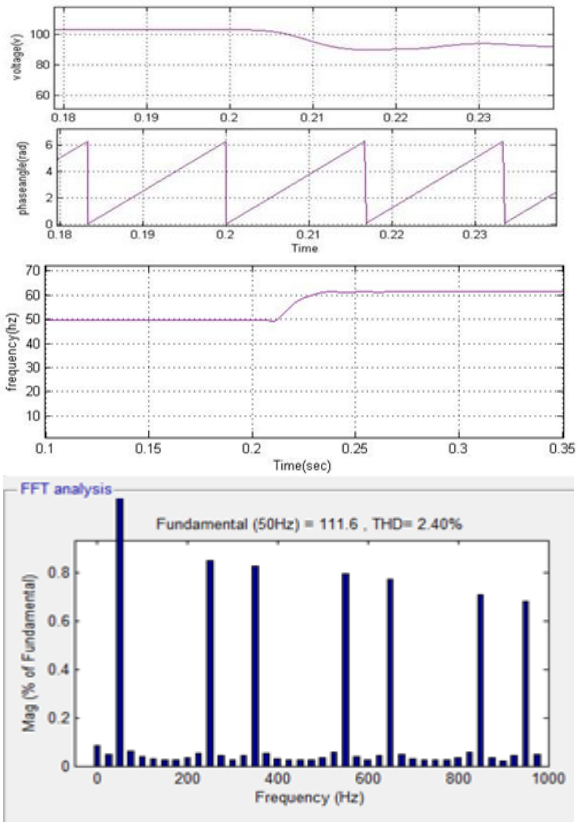

(a)) DDSRF PLL

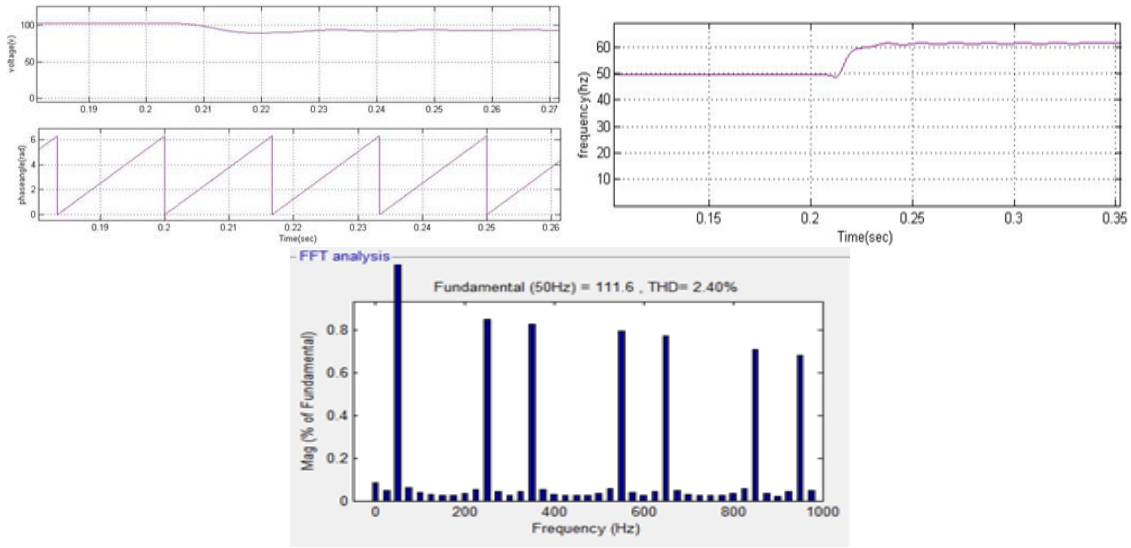

(b) DSOGI PLL

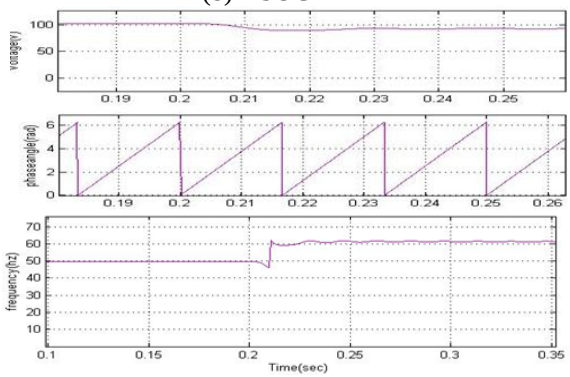

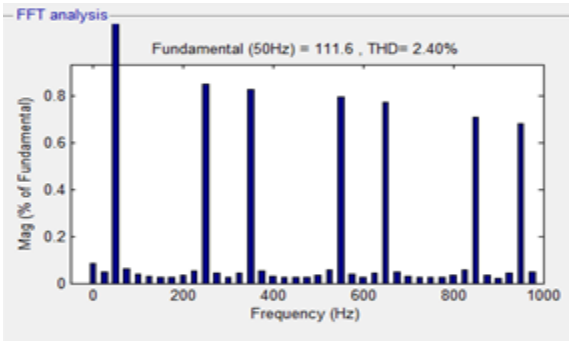

(c) EPLL

Fig. 21 Amplitude, phase, and frequency estimation for frequency changes
Behavior of PLLs in Case of Polluted Grid

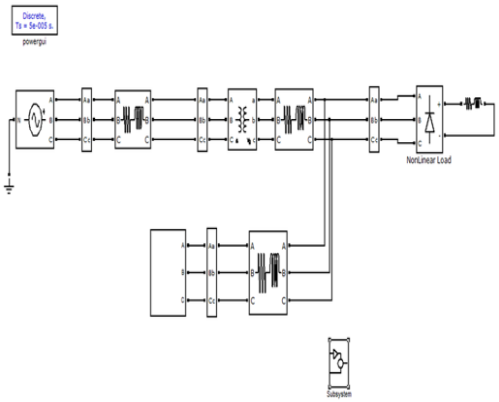

Fig. 22 General Distribution system when polluted grid

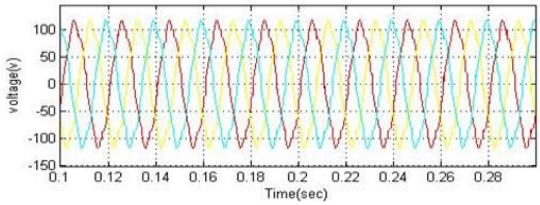

(a) Inputsignal (v)

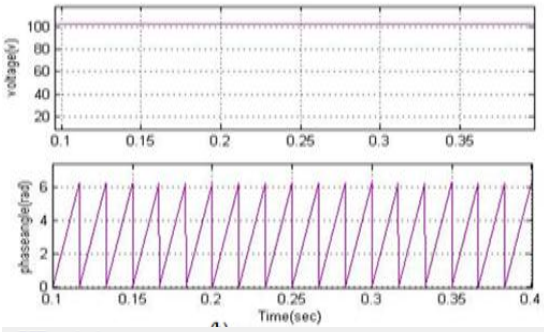

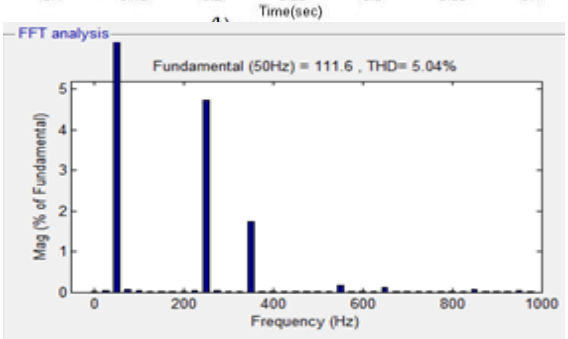

(b) DDSRF PLL

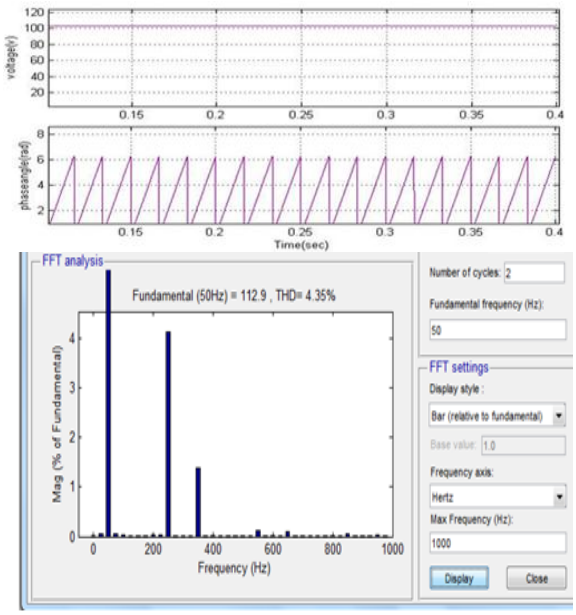

(c) DSOGI PLL

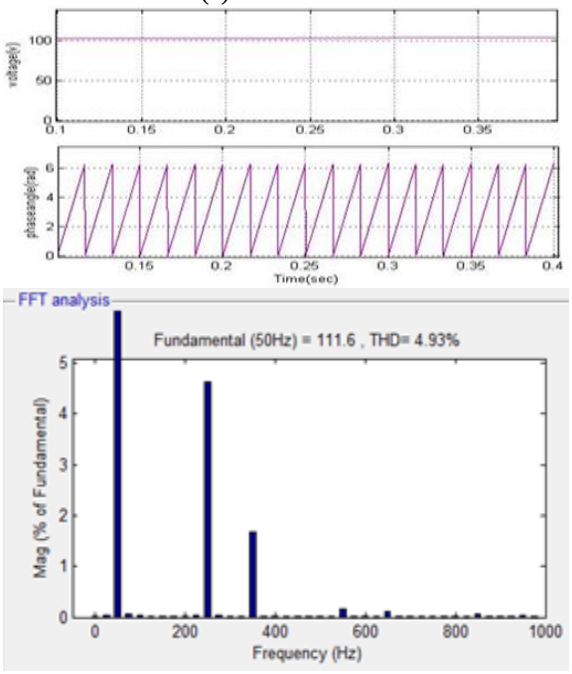

(c) EPLL

Fig.23 Amplitude (V) and phase detection (rad) for Polluted grid.

8. CONCLUSION

This project studied the behavior of threeadvanced grid synchronization systems by victimization fuzzy logic controller. Their structures are conferred, and their discrete algorithms are detailed. The immunity of the analyzed PLLs within the chance of a impure network is healthier once using the 3phEPLL and therefore the DDSRF, thanks to their bigger band pass and low-pass filtering capabilities. Here we tend to square measure victimization fuzzy logic controller rather than using different controllers. although the DSOGI also gives rise to reasonably sensible results, due to its inherent band pass filtering structure, its response is more full of harmonics. though all three are shown to be applicable for synchronizing with the network voltage in distributed power generation applications, primarily PV and wind generation, the lower computational value of the DDSRF PLL and theDSOGI PLL, in conjunction with their sturdy estimation of the voltage parameters, offers a more robust trade-off between the conferred systems, creating them significantly appropriate for wind power applications. The simulation was done by victimization fuzzy logic controller.

REFERENCES

[1] M. Tsili and S. Papathanassiou, "A review of grid code technical requirements for wind farms," IET Renew. Power Gen., vol. 3, no. 3, pp. 308–332,Sep. 2009.
[2] F. Iov, A. Hansen, P. Sorensen, and N. Cutululis, "Mapping of Grid Fault sand Grid Codes," Risø Nat. Lab., Roskilde, Denmark, Tech. Rep. RisoeR-1617, 2007.
[3] A. Luna, P. Rodriguez, R. Teodorescu, and F. Blaabjerg, "Low voltage ride through strategies for SCIG wind turbines in distributed power generation systems," in Proc. IEEE PESC, Jun. 15–19, 2008, no. 1, pp. 2333–2339.
[4] Saravanan R, Manoharan PS, Kanagaraj T, 'PSO based UPQC for power quality improvement', International Journal of Applied Engineering Research ,Vol.10, No.5, (2015), pp.4514-4520.
[5] Saravanan R and Manoharan PS, , 'Neuro Fuzzy based UPQC for power quality improvement', Journal of applied sciences research ,Vol.11, No.19, (2015) pp. 97-101.
[6] Ramesh Thangavel Saravanan Ragavan , "Gsm Based Low CostSmart Irrigation System with Wireless Valve Control", International Journal of Sensors and Sensor Networks ,Vol.5, No.4,(2017) pp. 54-62.
[7] D. Xiang, L. Ran, P. J. Tavner, and S. Yang, "Control of a doubly fed induction generator in a wind turbine during grid fault ride-through," IEEE Trans. Energy Conservation., vol. 21, no. 3, pp. 652–662, Sep. 2006.
[8]Saravanan R and Manoharan PS, 'Performance analysis of UPQCfor power quality improvement', Applied mechanics and materials, Vol.573, (2014), pp.690-695.
[9] Saravanan R,T.Ramesh, Manoharan P.S, and Muthuramalingam M"Dynamic Voltage restorer Application for Power Quality improvement in nonlinear load', International Journal of ResearchVol.4, No.17, (2017) pp. 3155-3161.
[10] Saravanan R & Manoharan PS, "Power quality improvement using UPQC based on particle swarm optimization", Bulletin ofElectrical Engineering and Informatics, Vol.2, No.1,(2013), pp.29-34.
[11]R Saravanan and P.S Manoharan , "Mitigation of voltage disturbances using DVR on distribution system with distributed generation", International Journal of Power Systems and Power Electronics,Vol.3, No.1,(2013), pp.49-56.